Skeletal Radiology (2019) 48:395–404
https://doi.org/10.1007/s00256-018-3043-0

SCIENTIFIC ARTICLE

High-resolution ultrasound in the assessment of the distal biceps brachii tendinous complex

M. Blasi[1,2] · J. De la Fuente[3] · A. Pérez-Bellmunt[2] · O. Zabalza[4] · S. Martínez[5] · O. Casasayas[2] · M. Miguel-Pérez[6,7]

Received: 4 May 2018 / Revised: 23 July 2018 / Accepted: 1 August 2018 / Published online: 5 September 2018

Abstract

Objective To establish a high-resolution US technique that enables a systematic morphometric examination of the three components that form the distal biceps brachii tendinous complex; the internal bicipital aponeurosis, the distal biceps brachii tendon and the external bicipital aponeurosis (also known as *lacertus fibrosus*).

Materials and methods Fifty cryopreserved cadaver body donor elbows were dissected to obtain morphometric reference values and to establish reliable landmarks for the US examination. Then, a systematic US technique was designed and validated by a one-to-one US/dissection analysis of 11 cryopreserved cadaver body donor elbows. Finally, the systematic US technique was carried out in 44 healthy volunteers and morphometric parameters were compared to those obtained in the first part of the study.

Results Mean dissection reference values: internal bicipital aponeurosis width 39.61 mm (10.02 SD) and thickness 0.75 mm (0.24 SD), distal biceps brachii tendon width 8.38 mm (1.87 SD) and thickness 2.73 mm (0.69 SD), external bicipital aponeurosis width 11.17 mm (5.84 SD) and thickness 0.85 mm (0.28 SD). One-to-one US/dissection correlation was overall good (intraclass correlation coefficient 0.876, $p < 0.0001$). When comparing volunteer US/dissection measurements, significant differences were encountered in all measures except for internal bicipital aponeurosis width. However, the overall magnitude of such significant differences was < 0.7 mm.

Conclusions Using the systematics hereby proposed, high-resolution US is reliable for the morphometric assessment of the distal biceps brachii tendinous complex. The external bicipital aponeurosis is morphometrically the most variable structure.

Keywords Distal biceps brachii tendon · Lacertus fibrosus · External bicipital aponeurosis · Internal bicipital aponeurosis · Ultrasound imaging

✉ M. Miguel-Pérez
mimiguel@ub.edu

[1] Department of Fundamental Care and Medical-Surgical Nursing, Faculty of Medicine and Health Sciences (Bellvitge Campus), University of Barcelona, Barcelona, Spain

[2] Àrea d'Estructura i Funció del Cos Humà, Facultat de Medicina i Ciències de la Salut, Universitat Internacional de Catalunya, Barcelona, Spain

[3] Orthopedic Department, Clínica Pakea-Mutualia, San Sebastián, Spain

[4] Unidad de análisis y apoyo a la investigación de Mutualia, Hospital Alta Resolución-Mutualia, Vitoria, Spain

[5] Radiology Department, Hospital Universitario de Burgos, Burgos, Spain

[6] Human and Embryology Anatomy Unit, Experimental Pathology and Therapeutic Department, Faculty of Medicine and Health Sciences (Bellvitge Campus), University of Barcelona, Barcelona, Spain

[7] Hospitalet de Llobregat, Feixa Llarga s/n, 08907 Barcelona, Spain

Introduction

High-resolution ultrasound (US) and magnetic resonance imaging (MRI) have been widely evidenced to be good tools in the assessment of the morphometric characteristics of the distal biceps brachii tendon (DBBT) normal anatomy and its associated pathology [1–9]. The DBBT is hyperechogenic and ovoid; it has two main components corresponding to the continuation of the short (SH) and long (LH) head biceps brachii myotendinous junctions. As the tendon transitions to deeper planes towards its attachment at the radial tuberosity, it rotates 90° and the DBBT LH becomes deep to the DBBT SH [3–6, 9, 10].

However, the distal attachment of the biceps brachii is not only composed of the DBBT but also by a bicipital aponeurotic expansion commonly known as bicipital aponeurosis or *lacertus fibrosus* [10–12]. These two components arise from a hyperechogenic intramuscular aponeurosis or flat tendon that originates within the center line of the biceps brachii muscle belly, spanning an average of 34% of the total

muscle length [10, 13]. To differentiate the bicipital aponeurosis or lacertus fibrosus from the intramuscular aponeurosis, from this point we refer to the first as the external bicipital aponeurosis (EBA) and to the latter as the internal bicipital aponeurosis (IBA). Also, we further refer to all three tendinous components mentioned of the distal biceps brachii aspect as the distal biceps brachii tendinous complex (DBBTC).

The EBA is very prone to anatomic variation in terms of morphologic and morphometric characteristics [9, 14–16]. Anatomically, it commences at the most medial and distal aspect of the DBBTC myotendinous junction and is composed of three layers [11, 17]. All three layers tend to progressively fuse together. Distally, the EBA progressively separates from the DBBT with an angulation of about 21° [17] and spans to fuse to the deep fascia and epimysium of the medial elbow muscle mass [11].

Although evidence exists that the EBA can be visualized by both MRI and US [1, 4, 10, 18, 19], to our knowledge there are no studies that characterize the US imaging morphometric characteristics of such structure, which would be important to fully elucidate its role in the clinical setting; specially in its implication in DBBT traumatic injuries [8, 20–22] and brachial vascular and median nerve entrapment syndromes at the elbow [23–25].

The aim of the present study is to establish whether the different components of the DBBTC (DBBT, IBA, and EBA) can be systematically examined by US and to propose a high-resolution US technique that is feasible and reproducible in a clinical setting to further be used to study pathologies affecting the DBBT, IBA, and or EBA.

Materials and methods

The present study was divided into three sequential parts. The first two parts intended to set the fundaments for the third part as they aimed to establish and validate a systematic US exploration. The third part aimed to translate this knowledge into an "in vivo" setting.

Gross anatomy morphometric characterization of the DBBTC

Fifty cryopreserved upper limbs from specimens (aged 67–89) with no apparent signs of pathology or previous surgery were left to thaw at normal room temperature for further dissection. All specimens derived from liberal donation to the Faculty of Medicine and Health Sciences (Bellvitge Campus), University of Barcelona.

The elbows were stratigraphically dissected until the whole biceps brachii was exposed. Afterwards, the EBA was sectioned at its most distal attachment site, at the level of the forearm deep fascia and the medial epicondylar muscle mass. Then, the DBBT was carefully detached from the radial tuberosity. Finally, the biceps brachii muscle fibers and paratenon were carefully dissected away, leaving only the core DBBTC components remaining.

After dissection, two different observers blinded to each other's work and using a Mytutoyo ABSOLUTE Solar Caliper Series 500 with ABSOLUTE technology (United States), performed the following measurements (Fig. 1):

- Level #1 IBA-thickness (IBA-t) and IBA-width (IBA-w) measurements: maximum transverse section of the IBA.
- Level #2 DBBT-thickness (DBBT-t) and width (DBBT-w) measurements: just distal to the distal myotendinous junction as the DBBT became an oval shaped tendon with two components (the DBBT SH and LH).
- Level #3 EBA-thickness (EBA-t) and EBA-width (EBA-w) measurements: just distal to the distal myotendinous junction still in continuation, parallel and medial to the DBBT SH.

During dissection, anatomic variations and pathological alterations where also considered and reported if found.

US systematic technique validation

Eleven additional cryopreserved upper limbs from specimens (aged 69–85) with no apparent signs of pathology or previous surgery were left to thaw at normal room temperature to be further studied. All specimens derived from liberal donation to the Faculty of Medicine and Health Sciences (Bellvitge Campus), University of Barcelona.

First all elbows were examined by US using a General Electric Logiq P6 ultrasound machine Korea, LTD, equipped with a high-frequency linear transducer (5–12 MHZ) and measured at the three levels specified on the previous subsection of the Materials and methods. Afterwards, they were dissected and measurements were repeated under direct vision, as specified on the previous subsection of the Materials and methods section. Anatomic variations and pathological alterations were also considered and reported if found.

US examination was performed in the short-axis view using the anterior approach [4, 26]. The transducer was placed on the muscle belly of the biceps brachii muscle, at the mid-third of the anterior arm, and it was shifted distal until the IBA was visible (Fig. 1). Then it was continued to shift distal until the transition to the DBBT and the EBA was visible (Fig. 1). To enhance the DBBT or EBA views, the transducer was centered on the DBBT and analyzed down to its attachment on the radial tuberosity. After, this was repeated but with the transducer centered on EBA.

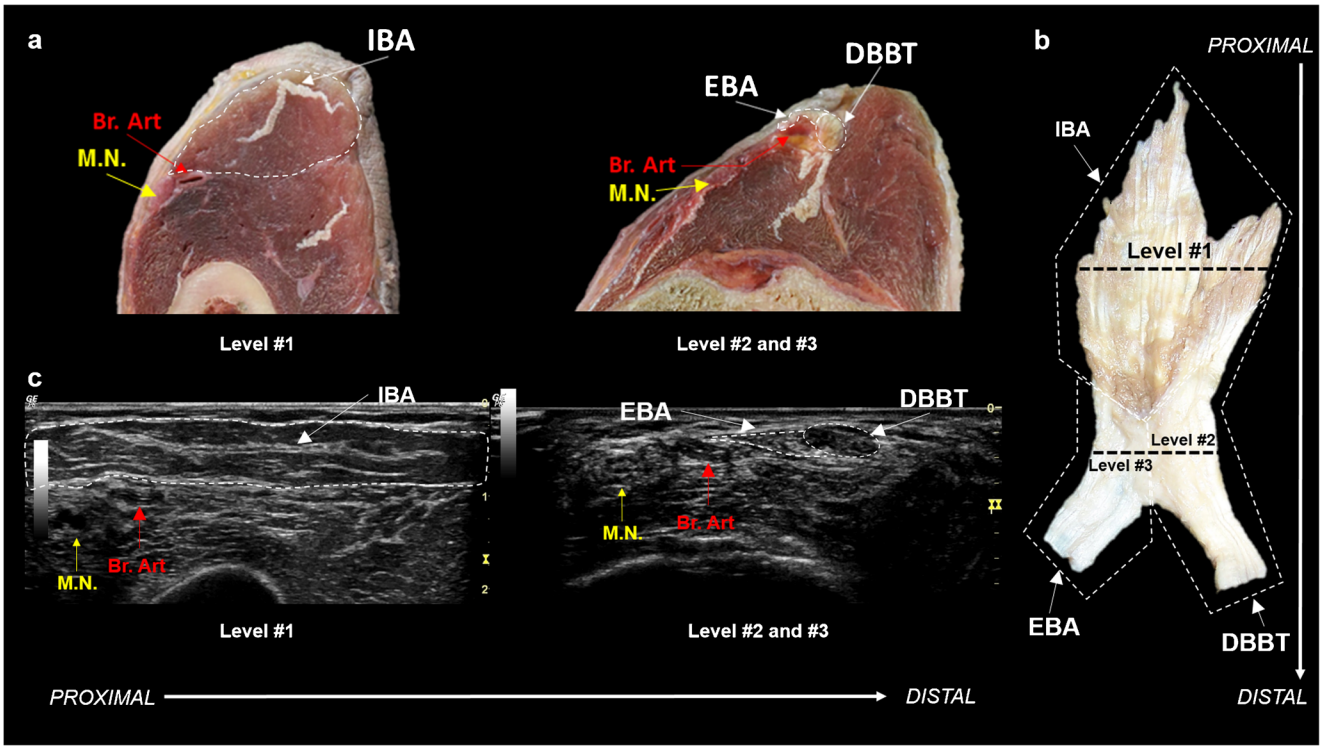

Fig. 1 DBBTC gross anatomy and US. **a** Gross anatomy cross sections obtained for illustrative purposes, **b** panoramic view of the DBBTC and **c** US short-axis sections of the elbow. Levels #1–3 of measurement are specified. Internal bicipital aponeurosis (IBA), external bicipital aponeurosis (EBA), distal biceps brachii tendon (DBBT), myotendinous junction (MTJ), braquial artery (Br. Art), braquial artery branching (Br. Art*), median nerve (M.N.)

Healthy volunteer US morphometric characterization of the DBBTC

Forty-seven volunteers who met the inclusion criteria from one of the following groups were recruited for this part of the study:

- Group 1: semi-professional tennis players. High and intense elbow-related activities on a daily basis.
- Group 2: cleaning and maintenance personnel. High but not intense elbow-related activities on a daily basis.
- Group 3: office personnel. Low intense elbow-related activities on a daily basis.

Three out of 47 volunteers were excluded as they also met some of the exclusion criteria:

- Previous history of traumatic injury with distal biceps brachii involvement or other previous pathology concerning the distal biceps brachii diagnosed by a doctor.
- Previous history of elbow surgery.

All volunteers completed a written informed consent according to the Clinical Research Ethics Committee from the University of Barcelona.

After acceptance, all 44 volunteers left underwent a bilateral US examination and measurement of the DBBTC according to the protocol specified on the previous subsections of the Materials and methods. For this purpose, we used a portable US Aloka Prosound C3 15.4" TFT monitor equipped with a high-frequency linear transducer (UST-TL01, 12L5).

Statistical analysis

Statistical analysis was performed using the IBM® SPSS Statistics® pack. For the "Gross anatomy morphometric characterization of the DBBTC" subsection, basic descriptive statistics were calculated. Agreement between two observers' measurements was analyzed with the intraclass correlation coefficient (ICC), or with the Kendall test if the data did not meet criteria of normality and homogeneity of variances.

For the "US systematic technique validation" subsection, basic descriptive statistics were calculated and agreement between the measurements obtained first during US exam (one examiner) and then the measurements obtained upon dissection (one observer) were analyzed with the ICC (US/dissection measurement agreement).

For the "Healthy volunteer US morphometric characterization of the DBBTC" subsection, a more detailed statistical analysis was performed. To compare measurements between dominant and non-dominant upper limbs, Student's *t* test

was used when the conditions of application allowed it, and the Wilcoxon test when the distribution was not normal.

To compare measurements between males and females, Student's *t* test was used when the conditions of application allowed it, the Welch correction when the variances were not homogeneous, and the Mann–Whitney test, when the distribution was not normal.

To see if there were significant differences between the three groups (1, 2, and 3), analysis of variance was done using the ANOVA test, when the conditions of normality and variance homogeneity allowed it, or the Welch correction (non-homogeneous variances) and the Kruskal–Wallis test (nonparametric) when the distributions did not conform to the normal distribution. Afterwards, the Tukey HSD test was done to identify the significance of the differences two-to-two.

Results

Gross anatomy morphometric characterization of the DBBTC

The DBBT attachment morphometric parameters and the ICC obtained by comparing the dissection measurements made by each of the two observers are specified in Table 1. The overall morphometric relation between the DBBT and EBA was very variable, as one could be larger than the other or vice versa (Fig. 2). The concordance analysis between observers ranged from excellent (ICC 0.969, $p < 0.0001$) to moderate (ICC 0.665, $p < 0.0001$) (Table 1).

From a morphologic point of view, the IBA was observed in all cases as a white flat and thin but fibrous intramuscular aponeurosis that had a rhomboidal-like shape on the frontal plane. Its lower vertex transitioned to form a white lateral ovoid-shaped tendon, the DBBT, and a medial white flat extramuscular aponeurosis that progressively separated in a fan-like manner from the latter, the EBA. Before removing the muscle fibers, the epimysium could be observed to be continuous over the DBBT and EBA conforming their paratenon. The paratenon was adhered to the proximal aspect of the DBBT and even macroscopic whitish collagen fibers could be observed directed diagonally towards the EBA (Figs. 1 and 2).

Six anatomic variants were noticed during the present study. Three biceps brachii muscles had supernumerary heads converging on the IBA-EBA transition. One biceps brachii distal attachment with a thin aponeurotic expansion from the EBA to the brachialis anterior muscle. One biceps brachii distal attachment had an aponeurotic expansion arising from the DBBT SH paratenon to the lateral forearm muscle compartment, mimicking a lateral EBA. In one of the biceps brachii, no fibers could be observed arising from the IBA to conform the EBA, which was strictly composed of the connective tissue arising from the biceps brachii epimysium and DBBT paratenon.

Although no apparent signs of elbow pathology were identified upon cadaver elbow selection, in one of the specimens a DBBT with chronic alteration signs was observed upon dissection. In this specimen, the DBBT presented degenerative changes as well as intratendinous calcifications at the free-tendon portion. Also, distally, the DBBT SH component was torn and detached from the radial tuberosity. Cortical alterations at the radial tuberosity were also observed in this specific specimen. The bicipital aponeurosis was macroscopically thicker and more fibrous than in the other cases studied, and its thickness value was among one of the thickest; 1.32 mm.

Table 1 Morphometric parameters measured by two observers and ICC

	IBA w		IBA t		DBBT w		DBBT t		EBA w		EBA t	
n	Obs. 1 50	Obs. 2	Obs. 1	Obs. 2	Obs. 1	Obs. 2	Obs. 1	Obs. 2	Obs. 1 49	Obs. 2	Obs. 1	Obs. 2
Mean (mm)	40.05	39.40	0.75	0.76	8.42	8.30	2.73	2.72	11.07	11.27	0.86	0.84
CI 95% inf	37.19	36.58	0.68	0.69	7.93	7.73	2.53	2.53	9.42	9.55	0.77	0.76
CI 95% sup	42.92	42.23	0.82	0.83	8.90	8.87	2.93	2.91	12.72	13.00	0.94	0.92
Median	39.47	38.66	0.74	0.73	8.23	8.47	2.62	2.70	9.96	9.76	0.83	0.80
SD	10.08	9.92	0.24	0.24	1.71	2.01	0.71	0.67	5.75	6.00	0.29	0.27
Minimum	24.82	24.49	0.33	0.36	5.54	1.54	1.20	1.27	2.69	2.87	0.44	0.27
Maximum	65.59	65.50	1.36	1.39	13.30	13.35	4.33	3.89	34.09	33.15	1.83	1.80
ICC	0.969		0.875		0.701*		0.868		0.861*		0.665*	
p value	$p < 0.0001$		$p < 0.0001$		$p < 0.0001$		$p < 0.0001$		$p < 0.0001$		$p < 0.0001$	
Interpretation	Excellent		Good		Moderate		Good		Good		Moderate	

Observer (Obs). * (Kendall's Tau-b coefficient, non-parametric)

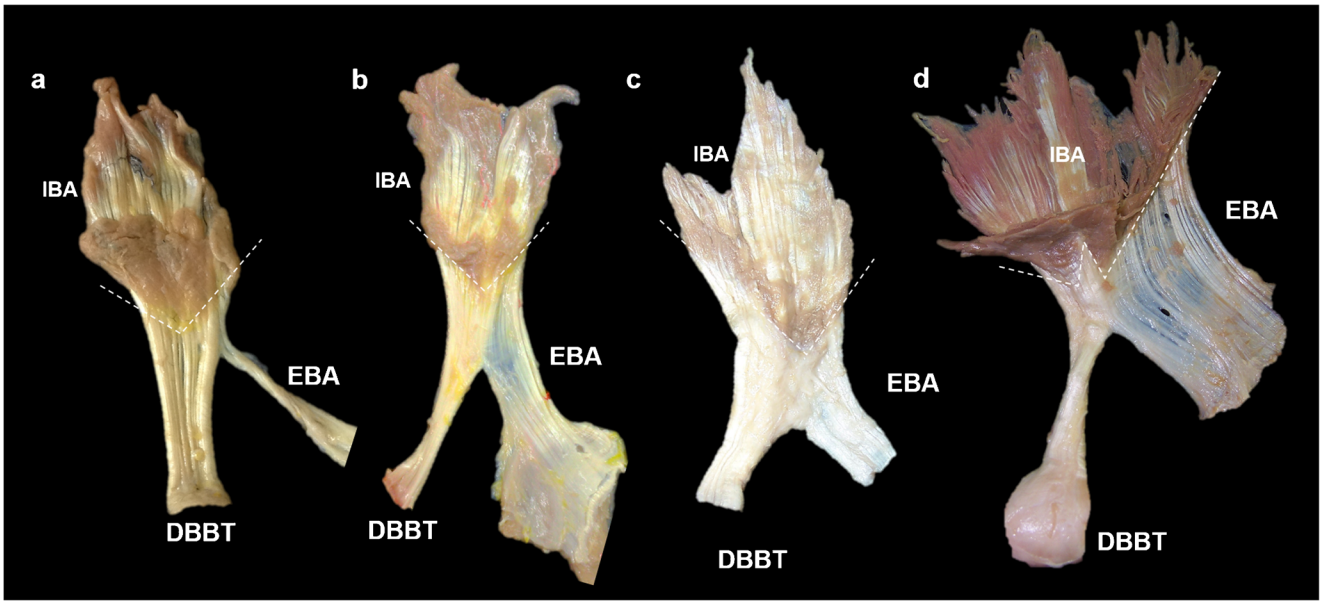

Fig. 2 Gross anatomy panoramic view of different types of DBBTC. **a**–**d** Biceps brachii muscle fibers have been removed in order to study the IBA, DBBT, and EBA, and so the distal myotendinous junction limits can be observed (*dashed lines*). From (**a**) to (**d**) the EBA becomes larger compared to the DBBT

US systematic technique validation

The systematic US technique proposed achieved a good overall correlation on the one-to-one morphometric correlation (ICC 0.876, $p < 0.0001$). However, when considering the US/dissection measurement agreement by means of the ICC we observed some variability; from excellent (0.902 in EBA-thickness), to good (0.886 DBBT width and 0.740 in EBA width) or no agreement (0.133 IBA thickness and 0.175 DBBT thickness) (Table 2).

Morphologic correlation was excellent (Fig. 1). The IBA could be observed centered within the biceps brachii muscle as a thick hyperechogenic band. It had a proximal vertex that progressively increased its width distally, and then once maximum width had been reached, it progressively decreased again. The distal decrease in width was due to an increase of lateral thickness that accounted for DBBT formation. Medial thickness remained very similar throughout its length as it continued distal as the EBA. No supranumerary heads were noticed on US nor dissection in this part of the study. However different spatial distributions of the IBA could be observed as the DBBTC perimysium converged onto it (Fig. 3).

The distal DBBT could be observed as a hyperechogenic oval-shaped structure, with two components; LH and SH, enclosed by its paratenon just distal to the myotendinous junction (Figs. 1 and 4). It then rotated 90° and transitioned to deeper planes towards the radial tuberosity.

The EBA was also fully conformed just distal to the DBBTC myotendinous junction as the superficial and deep epimysium of the biceps brachii muscle converged just superficial and deep to the EBA, and a three hyperechogenic-layered band could be observed (Fig. 4). Its cross section varied from triangular to rectangular. It progressively angulated away from the DBBT and fused to the deep fascia. The medial limit was sometimes difficult to locate as the brachial artery was just deep to it and the brachial pulse artifact altered the image. The brachial artery, veins, and median nerve could also be observed running deep to the EBA as it reached the level of the pronator teres (Figs. 1 and 4).

Just after the myotendinous junction, anisotropy helped to differentiate fibers to the DBBT from fibers to the EBA, as they had different trajectories (Fig. 1).

Table 2 US/dissection one-to-one comparison by means of the ICC

	All measurements	IBA w	IBA t	DBBT w	DBBT t	EBA w	EBA t
ICC	0.876*	0.557	– 0.133	0.886	0.175	0.740	0.902
p value	< 0.0001	0.0299	0.6603	0.0001	0.2933	0.0030	< 0.0001
Interpretation	Good	Moderate	Poor	Good	Poor	Good	Excellent

* (Kendall's Tau-b coefficient, non-parametric)

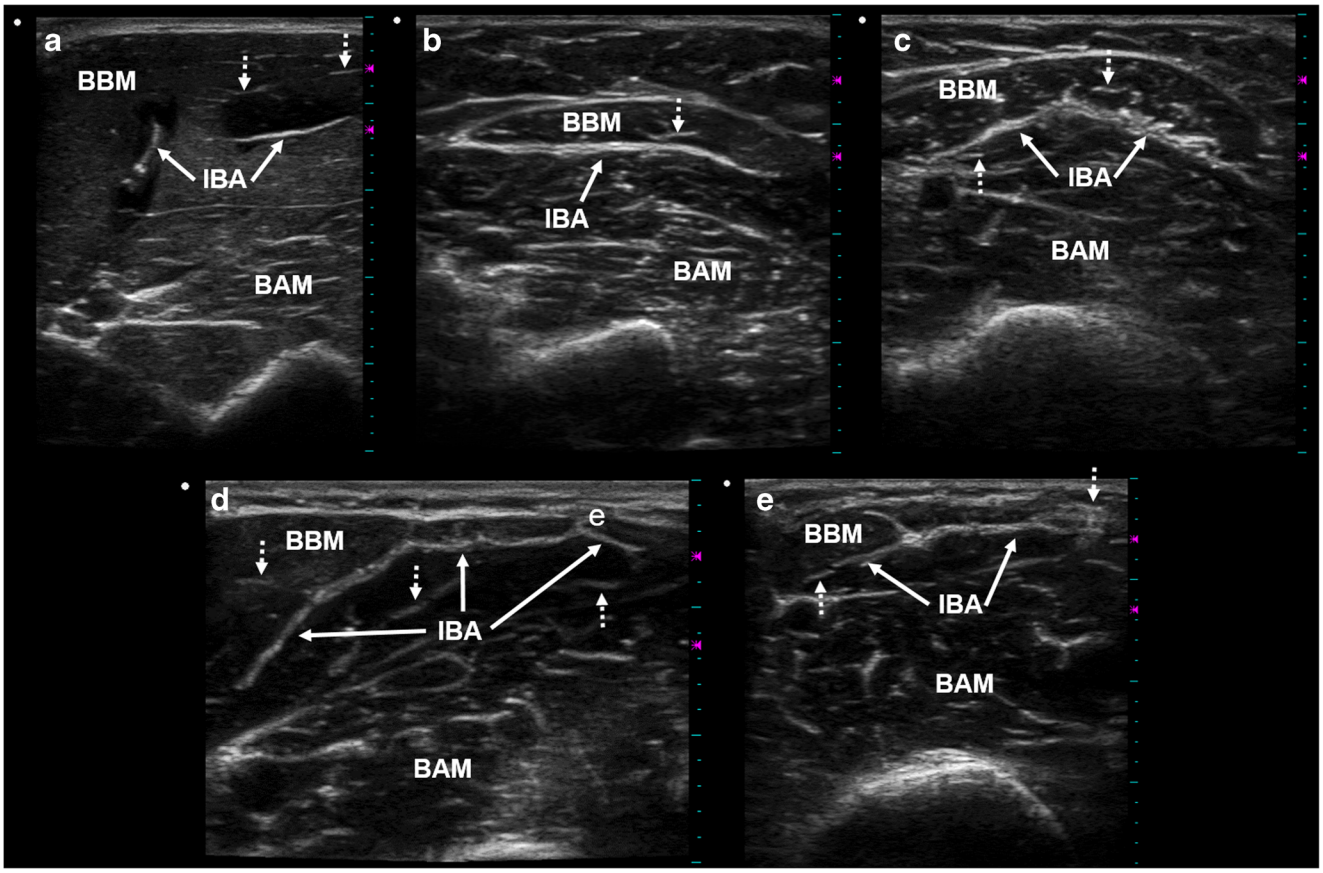

Fig. 3 Healthy volunteer US IBA patterns. **a** Proximally, the IBA had two components arising from the biceps brachii muscle LH and SH that fused distally. **b**–**e** A single wide IBA component was observed from its origin to the distal limit of the myotendinous junction. However, depending on how muscle fibers and the perimysium converged on the IBA, several three-dimensional morphologies were observed. Biceps brachii muscle (BBM), brachialis anterior muscle (BAM), perimysium thickenings (*dotted arrows*)

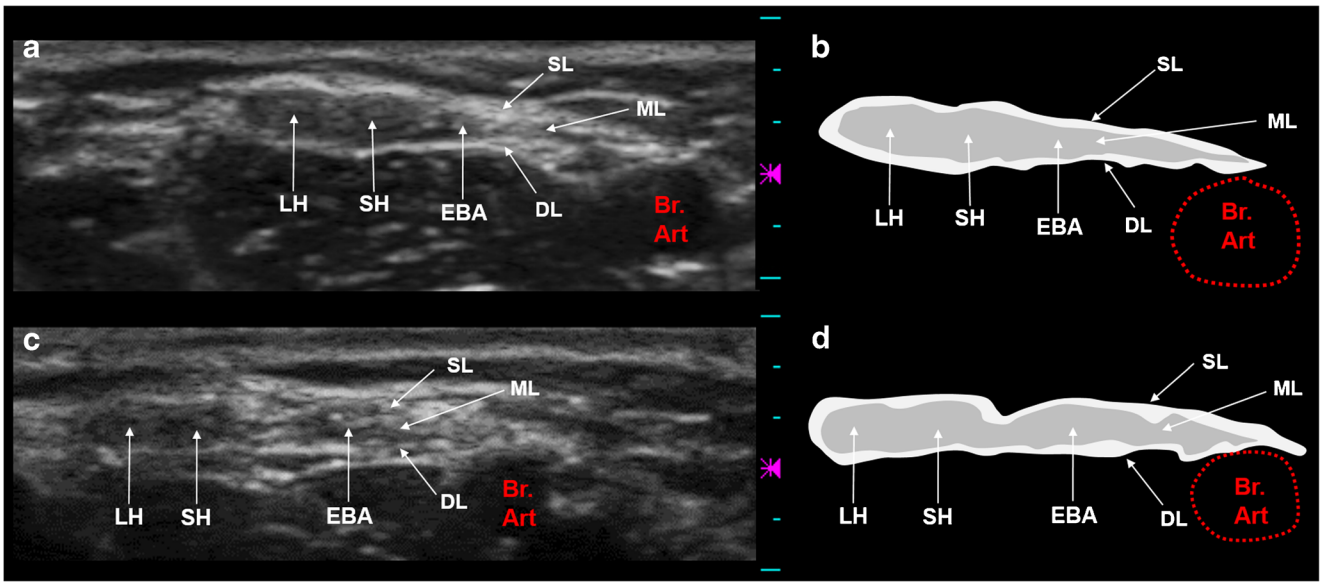

Fig. 4 Short-axis US zoom view of the DBBT LH, SH, and EBA. **a**–**d** The DBBT and EBA are surrounded by the same paratenon, hyperechogenic (**a** and **c**) and light grey (**b** and **d**), which is the distal continuation of the biceps brachii muscle epimysium. The three layers of the EBA can be distinguished; the paratenon forms de superficial layer (SL) and the deep layer (DL) while the middle layer (ML) corresponds to the distal extramuscular continuation of the IBA (**a**, **b**). Office personnel volunteer, the EBA is much smaller than the DBBT. **b**, **c** Semi-professional tennis volunteer, the EBA is much larger than the DBBT. Brachial artery (Br. Art)

Table 3 Volunteer characteristics

	Group 1	Group 2	Group 3	Total
Male	11	4	3	18
Female	4	12	11	27
Total	15	15	14	45
Age (mean)	17-1	51-9	52-4	40-5
Right dominant limb	14	14	14	42
Left dominant limb	1	2	0	3

Healthy volunteer US morphometric characterization of the DBBTC

Age, sex, dominant limb, and group according to level and intensity of DBBTC use at the workplace (groups 1–3) are specified in Table 3.

Significant differences were found between sexes, in IBA-w EBA-w, and EBA-t (Table 4). In all three measurements, the mean values obtained in men elbows were slightly larger than those obtained in women: IBA-w mean men 41.67 mm (SD 8.43)/women 34.95 mm (5.84 SD), EBA-w mean men 10.90 mm (3.54 SD)/women 8.37 (2.95 SD), EBA-t mean men 1.52 mm (0.54 SD)/women 1.31 mm (0.39 SD). When comparing dominant vs. non-dominant upper limbs (Table 4), significant differences were only obtained for IBA-t.

Significant differences were found for IBA-t, EBA-t, and DBBT-w. In the post-hoc tests, the following were found: i) significant differences for IBA-t between groups 1 and 2 and between groups 2 and 3, ii) significant differences for DBBT-w between groups 1 and 3, iii) significant differences for EBA-t between groups 1 and 2, between groups 1 and 3, and between groups 2 and 3 (Fig. 3, Table 5).

Table 5 Volunteer US comparison between level and intensity of elbow movements at the workplace

	p value					
Group 1 vs. 2	0.5968	< 0.0001	0.1229	0.9384	0.5975	0.0124
Group 1 vs. 3	0.6754	0.0988	0.0261	0.9301	0.8654	< 0.0001
Group 2 vs. 3	0.1754	0.0450	0.7658	0.7662	0.3123	0.0046

Comparison of results obtained on cadaver body donors versus US healthy volunteers

When comparing dissection gross anatomy measurements to US volunteer measurements, significant differences were noted for all measurements except for IBA width (Table 6). However, the magnitude of such differences when comparing CI of the following measures was acceptable; IBA-t, DBBT-w/t, EBA-t, was < 0.7 mm (Table 6). For EBA-w, the magnitude of the CI difference was < 2.3 mm. US overestimates dissection when measuring IBA-t and EBA-t and underestimates dissection in DBBT-w/t and EBA-w.

Discussion

The biceps brachii muscle distal aspect acts as an elbow flexor and forearm supinator. It may be injured after a sudden and intense extension force applied to the elbow when it is pre-set in an active flexed and supinated position [8, 27]. The incidence of DBBT ruptures is 1.2 injuries per 100,000 in the general population [27], with higher incidence rates registered in the active working population; 8.5 injuries per 100,000 [8]. The traumatic event acts on the whole DBBTC, however currently

Table 4 Volunteer US comparison between sexes and limb dominance

	IBA w		IBA t		DBBT w		DBBT t		EBA w		EBA t	
	Female	Male	Female	Male	Female	Male	Female	Male	Female	Male	Female	Male
n	54	34	54	34	54	34	54	34	54	34	54	34
Mean (mm)	34.95	41.67	0.9	0.83	7.92	7.86	2.19	2.18	8.37	10.90	1.31	1.52
CI 95% inf	33.35	38.72	0.85	0.78	7.53	7.15	2.04	2.01	7.57	9.66	1.20	1.37
CI 95% sup	36.54	44.61	0.95	0.88	8.31	8.58	2.34	2.35	9.18	12.14	1.42	1.68
SD	5.84	8.43	0.18	0.14	1.43	2.04	0.55	0.48	2.95	3.54	0.39	0.45
p value	0.0002		0.0696		0.6527		0.9500		0.0008		0.0219	
	Dom.	Non-D.	Dom.	Non-D.	Dom.	Non-D.	Dom.	Non-D.	Dom.	Non-D.	Dom.	Non-D.
n	44	44	44	44	44	44	44	44	44	44	44	44
Mean (mm)	37.76	37.33	0.91	0.84	8.02	7.78	2.28	2.09	9.04	9.66	1.37	1.42
CI 95% inf	35.20	35.24	0.85	0.79	7.46	7.31	2.12	1.94	8.03	8.59	1.23	1.29
CI 95% sup	40.33	39.42	0.96	0.89	8.58	8.24	2.44	2.25	10.04	10.73	1.50	1.55
SD	8.43	6.87	0.19	0.15	1.84	1.51	0.53	0.51	3.30	4.60	0.43	0.42
p value	0.5646		0.0092		0.6047		0.1044		0.4806		0.4178	

Dominant limb (Dom.). non-dominant limb (Non-D.)

Table 6 Dissection/volunteer US comparison

	IBA w		IBA t		DBBT w		DBBT t		EBA w		EBA t	
	Diss.	Vol.	Diss.	Vol.	Diss.	Vol.	Diss.	Vol.	Diss.	Vol.	Diss.	Vol.
n	98	88	98	88	98	88	98	88	98	88	98	88
Mean	39.61	37.54	0.75	0.87	8.38	7.90	2.73	2.18	11.17	9.35	0.85	1.39
CI 95% inf	37.60	35.92	0.70	0.83	8.00	7.54	2.59	2.07	10.00	8.63	0.79	1.30
CI 95% sup	41.62	39.17	0.80	0.91	8.76	8.26	2.87	2.30	12.34	10.07	0.90	1.48
Median	38.53	36.85	0.73	0.86	8.40	7.70	2.70	2.15	9.93	8.80	0.83	1.40
SD	10.02	7.65	0.24	0.17	1.87	1.68	0.69	0.52	5.84	3.41	0.28	0.43
Minimum	24.49	23.70	0.33	0.50	1.54	5.00	1.20	1.10	2.69	3.50	0.27	0.70
Maximum	65.59	63.80	1.39	1.34	13.35	13.50	4.33	3.50	34.09	19.50	1.83	2.40
Comparison of means (*p* value)	0.0916		0.0002		0.0253		< 0.0001		0.0438		< 0.0001	

Dissection (Diss.), Volunteer (Vol)

the study of these injuries has been mainly focused on the DBBT. Whether the EBA or the IBA remain unaltered or not in these injuries, what their role is after the injury has occurred or if EBA may play a direct role in other less frequent pathologies of the anterior elbow [23–25] is still to be determined.

The IBA can be only observed by means of imaging [10–13] or if the biceps brachii muscle fibers are carefully removed during dissection. Its location, centered within the biceps brachii muscle bellies, enables to increase the surface of the muscle–tendinous interface and is crucial to economize force transmission. The aponeurotic fibers of the IBA run parallel to each other and always converge laterally to conform an ovoid shape and finally constitute the DBBT, and medially they maintain its aponeurotic or flattened morphology to finally emerge from the muscle belly and constitute the EBA. Moreover, the position and morphology of the IBA conditions muscle architecture as muscle fibers must progressively converge on its surface. Consequently, when muscle fibers shorten heterogeneously during muscle contraction, they transmit force heterogeneously onto the IBA [13], favoring the hypothesis that the different components of the DBBTC have a certain degree of functional independence [4, 11].

Occasionally, a supernumerary biceps brachii muscle head contributes to conform the myotendinous junction on the EBA side [28]. We did not find any of these variants in the one-to-one comparison and therefore we cannot say whether US is reliable in identifying them. Nonetheless, several US types of IBA morphologies where identified. Moreover, the results obtained for one-to-one comparison in IBA measurements were the worst compared to DBBT and EBA measurement correlations (Table 2). Since we had to remove muscle fibers with a scalpel in order to perform gross anatomy dissection measurements, it is possible that the IBA was partially damaged (although not macroscopically obvious) and dissection measurements were not as accurate as those obtained by US in which the IBA remained unaltered at the moment of measurement.

For overall DBBT-w/t, the present study (Table 6) has obtained similar results as those previously reported on two smaller series of cadaver elbows (mean w 9.84–11.2 mm, SD 2.6–2.4 / mean t 3.32–4.8, SD 0.8–0.8) [10]. Moreover, we present US DBBT-w/t measurements in a series of 44 healthy volunteers (Table 6). One-to-one comparison was good for DBBT-w (ICC 0.886, *p* 0.0001) but poor for DBBT-t (ICC 0.175, $p = 0.2933$). This might have been due to the fact that when presenting the DBBTC on the dissection table to perform the measurements, the tendon was dis-rotated, as its normal distribution is helicoidal, describing a 90° external rotation from the myotendinous junction to its attachment on the radial tuberosity [10, 29]. Furthermore, US also enables the measurement of both DBBT components independently; 7.2 mm^2 for the LH and 5.6 mm^2 for the SH [4]. This brings up a fact that was also pointed out in dissection studies [11], and it is that the LH component of the DBBT occupies most of the radial tuberosity footprint.

The EBA is formed by three layers that progressively merge together and become continuous with the deep fascia of the forearm [11]. Our results support that the middle layer is the direct continuation of the IBA and conforms the EBA itself. We do report a high variability mainly in terms of EBA-w (Table 6) compared to the other measurement sites, however we doubt that it is a rudimentary layer [11], as it can be even wider than the DBBT. To our interpretation, the most superficial and deepest layers are the superficial and deep distal continuations of the biceps brachii muscle epimysium and therefore part of the paratenon. As whether the most superficial layer is thicker than the middle one or that the deepest layer is the thinnest [11], we cannot contribute objectively, as we only measured the middle layer.

The first specific EBA US description consisted of two clearly distinguishable white lines enveloping a hypoechoic band [19]. However, no measurements or a comparative analysis was performed to corroborate such description. Our

results concerning the US imaging characteristics of the EBA differ from those previously published. As aforementioned, anatomically, the EBA has been described to possess up to three layers [10, 11], which could be identified by US using the systematic technique hereby proposed as three adjacent hyperechogenic layers. The EBA lateral limit was the DBBT, and as both structures eventually angulated away from each other [15], dynamic transducer tilting and anisotropy could help to further differentiate them. The EBA medial limit was observed as the superficial and deep layers converged mainly onto the forearm deep fascia. In this way, it is important to keep in mind that the whole EBA eventually fuses with the deep fascia and medial epicondylar muscle mass and therefore it may be easily misinterpreted with the latter. Our observational US-dissection comparison is backed by the one-to-one quantitative US-dissection measurement comparison in which we obtained an excellent EBA-t correlation (ICC 0.902, $p < 0.0001$) and a good EBA-w correlation (ICC 0.740, $p < 0.003$).

All and all, choosing reference points to systematize EBA-w measurement is difficult, not only by US but also in gross anatomy under direct vision as the EBA opens up distally in a fan-shape manner, which implies that EBA-w varies rapidly in short length differences. In a previous gross anatomy study [15], mean EBA-w values were obtained at different EBA points to obtain a perspective of EBA morphometry variation. At the most proximal point, the EBA-w reference value was found to be 0.9 cm (SD 0.4) and at the central point 1.2 cm (SD 0.4) [15]. Our gross anatomy measurements (mean EBA-w 1.11 cm, SD 0.58) are overall concordant, probably as they were performed at the point of EBA-DBBT bifurcation, which falls in between the measurement points aforementioned [15]. Also, we contribute with a new EBA morphometric reference value, the EBA-t (Table 6), to which our knowledge has not been reported elsewhere in the literature.

Biomechanically, the EBA plays a role in force transmission from the biceps brachii muscle to the forearm distributed in two main tensional directions, medially and longitudinally, in relation to the epicondylar muscle mass [14]. In this way, as in the present study, healthy volunteers were selected from three population groups with a different level and intensity of elbow flexion and supination implication in their day-by-day activities at their workplaces, we could observe that the EBA-t was the only parameter to have consistently significant differences when comparing all three groups in pairs (Table 5). Mean EBA-t for semi-professional tennis players was 0.16 cm (SD 0.04), for cleaning and maintenance workers 0.14 cm (SD 0.03), and for office workers 0.10 cm (SD 0.03).

Moreover, although no apparent pathological signs were observed when the cadaver elbow was selected, one DBBT was found to have chronic degenerative signs and a minor partial tear at the attachment (less than 50% of the tendon thickness affected; type 2A [8]). This elbow presented a thick and fibrous EBA qualitatively and one of the thickest quantitatively (0.13 mm).

All and all, there exists a possibility that adaptive changes in response to specific EBA force transmission requirements may occur in terms of EBA-t. This should be further studied and verified in larger and more epidemiological homogeneous populations of both patients with DBBT injuries and healthy volunteers.

Other limitations to the present study are as follows. Although a good imaging correlation and overall numerical and statistical correlations were obtained between US measurements and dissection measurements, we did not directly perform an interobserver correlation analysis for US measurements, which should be further considered in other studies. Also, for both the first and third parts of the study, 50 and 88 elbows were considered, respectively, but we only analyzed 11 on the second part of the study.

To conclude, the present results support high-resolution US using the systematics hereby proposed as a reliable tool to morphometrically examine the DBBTC components, especially the EBA. Also, the advantages of identifying the EBA in the clinical setting should be considered to further clarify controversies about its implication in DBBT injuries, whether it should be surgically repaired when torn [20, 21], the evaluation of the EBA as it may be used as a reconstruction graft in chronic distal biceps tears [22], and its role in median nerve and brachial vascular entrapment syndromes [23–25].

Acknowledgements The authors are thankful to body donors and volunteers that enable the study of basic and clinical anatomy. We also thank the dissection room staff: Josep Lluís Ramon, Gemma Ramon, Nieves Cayuela, Cristobal Martín and Alicia Rodrigo, for their help and assistance. Finally, we thank the Bruguera Tennis Academy for allowing us to examine elite tennis players and Mathias Simon for his assistance during data gathering.

Compliance with ethical standards

Conflict of interest The authors declare that they have no conflict of interest.

Ethical approval All procedures involving human participants were in accordance with the ethical standards of the Clinical Research Ethics Committee (CEIC).

References

1. Giuffre BM, Lisle DA. Tear of the distal biceps brachii tendon: a new method of ultrasound evaluation. Australas Radiol. 2005;49:404–6.
2. Festa A, Mulieri PJ, Newman JS, Spitz DJ, Leslie BM. Effectiveness of magnetic resonance imaging in detecting partial and complete distal biceps tendon rupture. J Hand Surg [Am]. 2010;35:77–83. https://doi.org/10.1016/j.jhsa.2009.08.016.

3. Smith J, Finnoff JT, O'Driscoll SW, Lai JK. Sonographic evaluation of the distal biceps tendon using a medial approach: the pronator window. J Ultrasound Med. 2010;29:861–5.
4. Tagliafico A, Michaud J, Capaccio E, Derchi LE, Martinoli C. Ultrasound demonstration of distal biceps tendon bifurcation: normal and abnormal findings. Eur Radiol. 2010;20:202–8. https://doi.org/10.1007/s00330-009-1524-1.
5. Brasseur JL. The biceps tendons: from the top and from the bottom. J Ultrasound. 2012;15:29–38. https://doi.org/10.1016/j.jus.2011.11.002.
6. Brigido MK, De Maeseneer M, Morag Y. Distal biceps brachii. Semin Musculoskelet Radiol. 2013;17:20–7. https://doi.org/10.1055/s-0033-1333910. Review
7. Champlin J, Porrino J, Dahiya N, Taljanovic M. A visualization of the distal biceps tendon. PM R. 2017;9:210–5. https://doi.org/10.1016/j.pmrj.2016.10.005.
8. de la Fuente J, Blasi M, Martínez S, et al. Ultrasound classification of traumatic distal biceps brachii tendon injuries. Skelet Radiol. 2018;47(4):519–32. https://doi.org/10.1007/s00256-017-2816-1.
9. Dirim B, Brouha SS, Pretterklieber ML, Wolff KS, Frank A, Pathria MN, et al. Terminal bifurcation of the biceps brachii muscle and tendon: anatomic considerations and clinical implications. AJR Am J Roentgenol. 2008;191:W248–55. https://doi.org/10.2214/AJR.08.1048.
10. Blasi M, de la Fuente J, Martinoli C, et al. Multidisciplinary approach to the persistent double distal tendon of the biceps brachii. Surg Radiol Anat. 2014;36:17–24. https://doi.org/10.1007/s00276-013-1136-y.
11. Eames MH, Bain GI, Fogg QA, van Riet RP. Distal biceps tendon anatomy: a cadaveric study. J Bone Joint Surg Am. 2007;89:1044–9.
12. Testut L, Latarjet A. Tratado de Anatomía Humana. 8th ed. Barcelona: Salvat Editores, S.A.; 1944.
13. Pappas GP, Asakawa DS, Delp SL, Zajac FE, Drace JE. Nonuniform shortening in the biceps brachii during elbow flexion. J Appl Physiol (1985). 2002;92:2381–9.
14. Stecco A, Macchi V, Stecco C, et al. Anatomical study of myofascial continuity in the anterior region of the upper limb. J Bodyw Mov Ther. 2009;13:53–62. https://doi.org/10.1016/j.jbmt.2007.04.009.
15. Snoeck O, Lefèvre P, Sprio E, et al. The lacertus fibrosus of the biceps brachii muscle: an anatomical study. Surg Radiol Anat. 2014;36:713–9. https://doi.org/10.1007/s00276-013-1254-6.
16. Nayak SB, Swamy RS, Shetty P, Maloor PA, Dsouza MR. Bifurcated bicipital aponeurosis giving origin to flexor and extensor muscles of the forearm—a case report. J Clin Diagn Res. 2016;10:AD01–2. https://doi.org/10.7860/JCDR/2016/17714.7215.
17. Joshi SD, Yogesh AS, Mittal PS, Joshi SS. Morphology of the bicipital aponeurosis: a cadaveric study. Folia Morphol (Warsz). 2014;73:79–83. https://doi.org/10.5603/FM.2014.0011.
18. De Maeseneer M, Brigido MK, Antic M, et al. Ultrasound of the elbow with emphasis on detailed assessment of ligaments, tendons, and nerves. Eur J Radiol. 2015;84(4):671–81. https://doi.org/10.1016/j.ejrad.2014.12.007. Review
19. Konschake M, Stofferin H, Moriggl B. Ultrasound visualization of an underestimated structure: the bicipital aponeurosis. Surg Radiol Anat. 2017;39:1317–22. https://doi.org/10.1007/s00276-017-1885-0.
20. Le Huec JC, Moinard M, Liquois F, Zipoli B, Chauveaux D, Le Rebeller A. Distal rupture of the tendon of biceps brachii. Evaluation by MRI and the results of repair. J Bone Joint Surg (Br). 1996;78:767–70. Erratum in: J Bone Joint Surg Br 1997 Jul;79(4):693
21. Landa J, Bhandari S, Strauss EJ, Walker PS, Meislin RJ. The effect of repair of the lacertus fibrosus on distal biceps tendon repairs: a biomechanical, functional, and anatomic study. Am J Sports Med. 2009;37:120–3. https://doi.org/10.1177/0363546508324694.
22. Murthi AM, Ramirez MA, Parks BG, Carpenter SR. Lacertus fibrosus versus Achilles allograft reconstruction for distal biceps tears: a biomechanical study. Am J Sports Med. 2017;45:3340–4. https://doi.org/10.1177/0363546517727511.
23. Nelson KR, Goodheart R, Salotto A, Tibbs P. Median nerve entrapment beneath the bicipital aponeurosis: investigation with intraoperative short segment stimulation. Muscle Nerve. 1994;17:1221–3.
24. Cevirme D, Aksoy E, Adademir T, Sunar H. A perplexing presentation of entrapment of the brachial artery. Case Rep Vasc Med. 2015;2015:236193. https://doi.org/10.1155/2015/236193.
25. Caetano EB, Vieira LA, Almeida TA, Gonzales LAM, Bona JE, Simonatto TM. Bicipital aponeurosis. Anatomical study and clinical implications. Rev Bras Ortop. 2017;53:75–81.
26. Kayser R, Mahlfeld K, Scheller W, Müller J, Schmidt W, Heyde CE. Sonographic imaging of the distal biceps tendon—an experimental and clinical study. Ultraschall Med. 2005;26:17–23.
27. Safran MR, Graham SM. Distal biceps tendon ruptures: incidence, demographics, and the effect of smoking. Clin Orthop Relat Res. 2002 Nov;(404):275–283.
28. Cucca YY, McLay SV, Okamoto T, Ecker J, McMenamin PG. The biceps brachii muscle and its distal insertion: observations of surgical and evolutionary relevance. Surg Radiol Anat. 2010;3:371–5. https://doi.org/10.1007/s00276-009-0575-y.
29. Kulshreshtha R, Singh R, Sinha J, Hall S. Anatomy of the distal biceps brachii tendon and its clinical relevance. Clin Orthop Relat Res. 2007;456:117–20.